CIMAC CONGRESS 25
ZURICH, MAY 19 – 23, 2025

2025 | 112

Research on methanol spray characteristics of marine engine

Fuel Injection & Gas Admission and Engine Components

Xinran Wang, China Shipbuilding Power Engineering Institute CO, Ltd

Teng Liu, China Shipbuilding Power Engineering Institute CO, Ltd
Shiyan Li, Shanghai JiaoTong University
Lei Cui, China Shipbuilding Power Engineering Institute CO, Ltd
Yuehua Qian, China Shipbuilding Power Engineering Institute CO, Ltd

ABSTRACT

Based on the International Maritime Organization's (IMO) zero-carbon shipping strategy by the end of this century, green and low-carbon ships will become the mainstream idea of future maritime development. From the evaluation of fuel availability and technology maturity, methanol fuel is a green and low-carbon marine fuel with commercial application at this stage. Low pressure inlet injection is the best form of methanol medium speed machine and has good technical maturity. However, due to the unknown characteristics of inlet methanol injection mixture, its coupling effect with inlet strong airflow has not been clarified, which seriously restricts the improvement of substitution rate and cycle variation in inlet methanol engine. Therefore, it is urgent to carry out relevant basic research on methanol fuel inlet injection, so as to clarify the methanol injection mixture characteristics of marine engine inlet, and the results can be used to guide the improvement of the accuracy of in-cylinder three-dimensional simulation.

To investigate the characteristics of methanol injection mixture in the intake port of marine engines and enhance the accuracy of in-cylinder three-dimensional simulations, an experimental study on methanol intake port spray was conducted. Based on a visualizable low-pressure constant volume combustion bomb test platform, optical methods such as high-speed background light scattering and microphotography were employed to explore the influence of ambient temperature and injection pressure on methanol spray cone angle, penetration distance, and particle size distribution under low-pressure methanol injection conditions in the intake port. The results showed that at lower temperatures, the impact of density changes caused by temperature variations in the spatial atmosphere was more significant than the temperature's promotion of methanol atomization. The influence of ambient temperature on the front end of the methanol spray was more significant than on the middle and lower sections, with the distribution of micro particle sizes mainly in the middle and lower sections. When the initial temperature increased by 50K, the front end of the methanol spray was significantly affected by the ambient temperature, and the distribution of micro particles became denser. In the middle section, the spray was primarily affected by the decrease in surrounding gas density. The interaction between methanol droplets and the surrounding air was minimal, limiting atomization, and the particle size distribution of small droplets was relatively uniform. Additionally, low-load conditions were more likely to cause wet-wall phenomena in methanol intake port sprays.

1 INTRODUCTION

Based on Chinese “3060” dual carbon targets and the International Maritime Organization's (IMO) strategy for zero-carbon shipping by or around 2050, the greening and low-carbonization of ships will become the mainstream approach for future maritime development [1]. Currently, hydrogen, ammonia, and methanol are recognized as typical zero-carbon fuels in the industry. From the perspectives of fuel availability and technological maturity evaluation, methanol fuel is a green and low-carbon ship fuel that is commercially viable at this stage [2].

In the field of marine engines, Europe's MAN has not only developed low-speed two-stroke engines with high-pressure methanol injection, achieving a substitution rate of 95%, but is also advancing the development of its L21/31 medium-speed engines with low-pressure intake port methanol injection, believing that low-pressure intake port injection is the optimal implementation form for methanol medium-speed engines. WinGD is expected to conduct the first phase of validation tests for methanol low-speed engines in 2024. Wärtsilä relies on its main 320 engine model to develop high-pressure dual direct-injection medium-speed methanol engines, with a maximum substitution rate of over 90%. Belgium's ABC has developed DZD medium-speed engines with low-pressure intake port methanol injection, achieving a maximum substitution rate of 70%. South Korea's Hyundai is also pursuing research and development in methanol marine engines, focusing on high-pressure dual direct-injection and low-pressure intake port ammonia fuel engines [3-5].

The spray combustion process within an engine cylinder not only influences its overall power performance and emissions but also plays a decisive role in factors such as thermal load and working pressure. Furthermore, the accuracy of spray simulation is crucial to the calculation results of simulation [6-8]. Pickett et al. [9] set up a visual constant volume combustion bomb. By studying the relationship between the diesel ignition delay in the combustion chamber and the flame lift length of spray combustion, it was found that the flame lift length decreased with the decrease of the ignition delay period. Edwards and Siebers et al. [10-11] carried out a large number of diesel spray ignition and combustion experiments under different working conditions based on the constant volume bomb, and found that the fuel spray first atomized along the edge under high temperature conditions, and then gradually evaporated and ignited to form a stable state. Fang et al. [12] simulated the combustion process of diesel spray under low-temperature environment based on constant volume combustion bomb, and found that the middle and downstream areas of the combustion flame were high temperature combustion prone areas. Dennis et al. [13] combined the laser induced fluorescence method with the constant volume combustion bomb device to obtain diesel spray combustion flame images under different working conditions, and found that the generation of soot and other particles is mainly related to the flame lift length in the combustion process. Jia Tao et al. [14] established a methanol engine combustion model through methanol spray calibration tests and found that the quasi-dimensional combustion model based on methanol chemical reaction mechanisms had relatively small errors compared to experimental data. The multi-dimensional combustion model for methanol engines had high calculation accuracy but requires significant computational resources. Xu Min et al. [15] analyzed the gas-liquid penetration phenomenon of spray combustion in diesel engine cylinder and the entrainment phenomenon of spray in confined space, and developed models for gas-liquid penetration and volume concentration distribution of the spray plume in a confined space.

Low-pressure intake port injection represents the optimal implementation for methanol medium-speed engines, characterized by a high level of technical maturity. However, due to the unclear characteristics of the methanol-air mixture in the intake port during injection, and the unclarified interaction between this mixture and the strong intake air flow, the improvement of substitution rates and the reduction of cycle variations in methanol-fueled engines are severely hindered. Therefore, it is urgent to carry out relevant basic research on methanol fuel intake port injection.

In this paper, a constant volume combustion chamber experimental platform is utilized to investigate the spray pattern and atomization characteristics of methanol intake port injection under static conditions, which provides theoretical and experimental support for future calibration of methanol spray model, improvement of accuracy of three-dimensional simulation in cylinder, and development of methanol medium speed engine technology.

2 EXPERIMENTAL SETUP

2.1 Low-Pressure Constant Volume Combustion Bomb

Figure 1 illustrates the constant volume combustion bomb employed in the experiment, which has a maximum pressure tolerance of 2.0 MPa and can be heated to a maximum ambient temperature of 423K. This bomb is capable of

simulating experiments related to the coupling of high-speed airflow during the engine's intake stroke with liquid or gaseous fuel sprays, with a maximum flow velocity reaching 150 m/s. The device is equipped with three optical windows for direct photography and optical diagnostics such as laser sheet lighting. Internally, it features inner and outer sleeves that can be adapted based on the actual diameter of an engine's intake pipe. It also includes a nozzle adapter module that allows for experiments with multiple types of nozzles. In front of the visualizable pressure vessel, there is a flow field rectifier cavity that can quickly stabilize high-speed airflow, achieving a uniform and stable high-speed flow field for visualization experiments. A throttle valve is installed downstream of the device, and by adjusting its opening, it can simulate experimental conditions with high intake backpressure typical of highly boosted engines. Additionally, the device can be converted into a general low-pressure constant-volume combustion bomb by removing the flow field rectifier, thereby serving multiple purposes. The basic experimental conditions include low backpressure, a heating temperature of only 350K, and static spray conditions. Therefore, for static spray experiments, the flow field rectifier is removed, retaining the visualizable pressure vessel to form a general low-pressure constant-volume combustion bomb.

Figure 1. Constant volume combustion bomb

2.2 Methanol Fuel Injection System

The methanol fuel injection device uses a piston pump to directly provide the injection pressure required for low-pressure methanol, as shown in Figure 2. The methanol injector used for the experiment is shown in Figure 3. The number of holes is 180 and the diameter is 0.35mm.

Figure 2. Low-pressure methanol fuel injection device

Figure 3. Methanol injector for experiment

2.3 Background Light Scattering and Microphotography

Figure 4 and 5 shows the arrangement of the Diffused Background Illumination (DBI) method used in the experiment for capturing the low-pressure static methanol spray, aiming to obtain the spatial development characteristics of the liquid phase of methanol fuel. During the experiment, the high-speed camera was set with an exposure time of 1 second, a resolution of 512 × 464 pixels, a shooting speed of 50,000 frames per second (fps), a lens focal length of 105mm, and an aperture of 2.0. Each experimental condition was filmed three times, and the experimental analysis adopted the average of these three measurements.

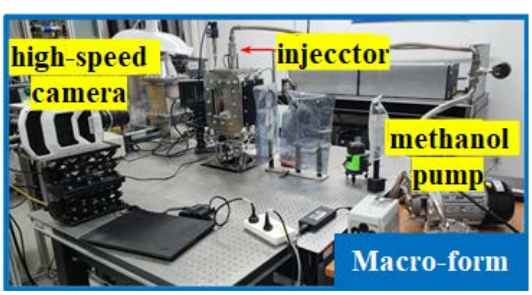

Figure 4. Experiment on macroscopic morphology

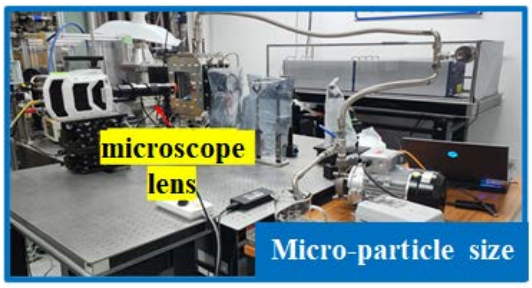

Figure 5. Microscopic particle size of methanol static spray

2.4 Experimental Conditions

Based on the visual bomb test-bed, taking the methanol injector as the object, the air temperature, pressure and methanol pressure were adjusted to reach the set value in the air static state to simulate the environment in the intake port of a cylinder diameter methanol fuel engine, and the methanol spray cone angle, penetration and particle size distribution were studied under different air pressure and temperature, different methanol injection pressure difference and pulse width. The cone angle, penetration distance and particle size distribution of methanol spray at different times were recorded by optical measurement. The test parameters of specific test points are shown in Table 1.

Table 1. Experimental conditions of methanol static spray

NO.	Air temperature/ K	Air pressure /barG	Methanol injection pressure/barG	Injection pulse width/ms
1	298	3	9	10
2	310	3	9	10
3	323	3	9	10
4	298	2	8	10
5	298	1	7	10

The overall workflow of the experiment is as follows. Firstly, design and fabricate an adapter suitable for the bomb according to the structural characteristics of the fuel injector, as shown in Figure 6. Then, conduct flow rate testing to obtain the corresponding fuel injector flow rate under the experimental pulse width. Finally, perform static macroscopic morphology testing; and perform static spray particle size testing.

Figure 6. Injector adapter

2.5 Injector flow rate test

Based on the test operating points in Table 1, measure the fuel injector flow rate under all operating conditions. The flow rate tests were conducted at normal temperature and pressure (injection pressure of 6 bar, ambient pressure of 0 bar, ambient temperature of 298K). The FA2004 electronic analytical balance, as shown in Figure 7, was used for weighing in the experiments.

Figure 7. Electronic balance for flow testing

3 PROCESSING OF EXPERIMENTAL RESULTS

3.1 Results of Macroscopic Morphology Testing and Image Data Processing

Through the macro morphology test results, we can know the overall spray profile of the fuel injector. Figure 8 shows the change results of the original picture of the macro morphology of the injector with time under the reference working conditions (injection pressure 9 bar, ambient pressure 3 bar, ambient temperature 298K).

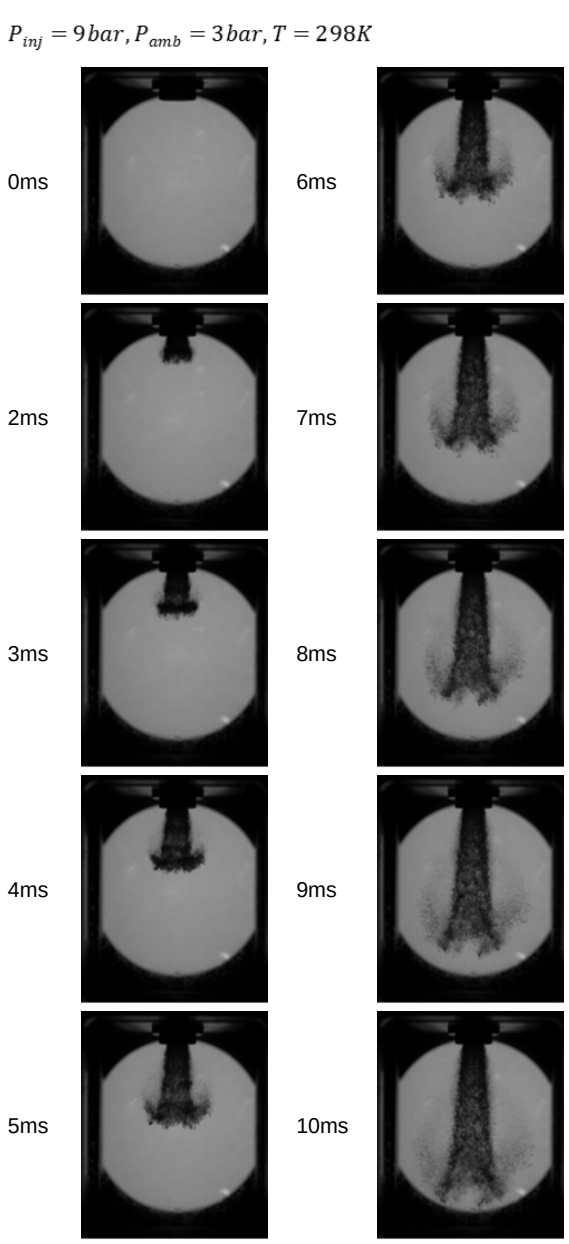

Figure 8. Original macroscopic morphology image of case1

Based on the macroscopic morphology test results, the image (5.0ms) was processed as shown in Figure 9. Firstly, subtract the background, crop out the relevant area, obtain the pure spray image, and perform binarization. What's more, based on the contour, obtain the spray penetration distance (65.0mm) and spray angle (18.4 degrees), and draw grid lines. Eventually, statistical analysis is conducted on the penetration distance and spray angle at different time points.

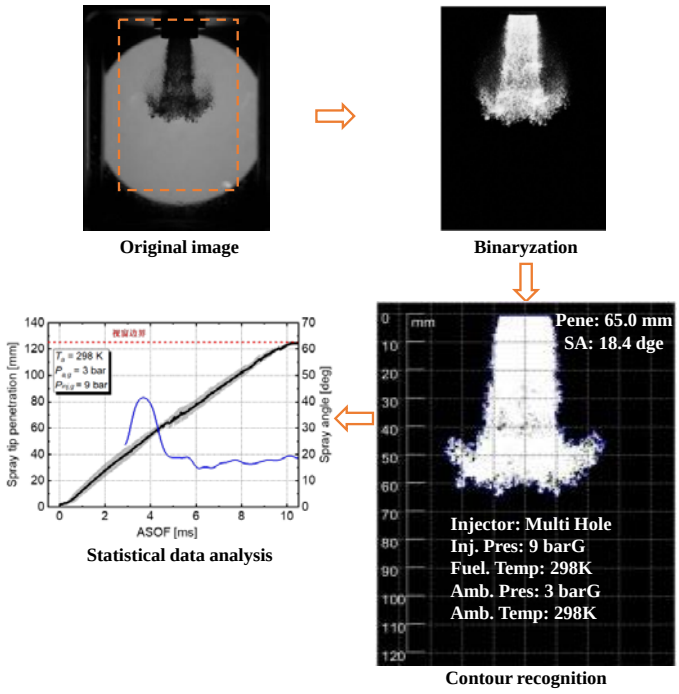

Figure 9. Processing flow for macroscopic morphology

For macroscopic characteristics, the definition of spray angle (SA) is illustrated in Figure 10. After the spray penetration distance exceeds 30mm, the outer contours at 10mm and 30mm below the nozzle are obtained and connected. The angle between the sloping sides of the resulting trapezoid is defined as the spray angle, which is in accordance with the SAEJ2715 standard.

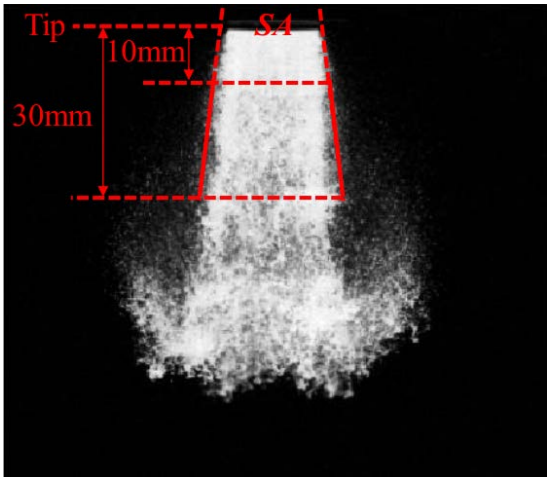

Figure 10. Schematic diagram defining macroscopic spray angle

3.2 Results of Particle Size Testing and Image Data Processing

In static experiments, particle size measurements were taken at two positions, 60mm and 80mm below the nozzle. Figure 11 shows the data

processing workflow: Firstly, sampling positions were selected based on the spray contour. Subsequently, a high-resolution camera was used to capture microscopic images, distinguishing between continuous liquid surfaces, droplets, and liquid bands. In the end, eligible droplets were identified and counted to obtain the droplet size distribution characteristics.

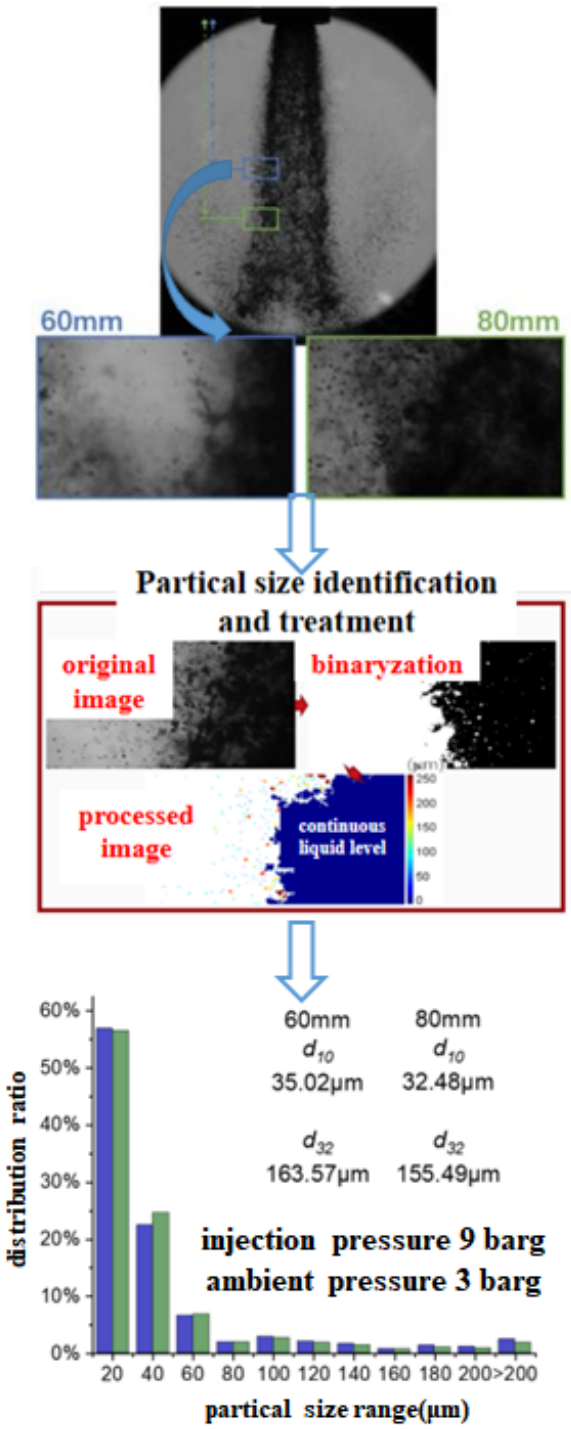

Figure 11. Flowchart for spray particle size processing

4 ANALYSIS OF SPRAY EXPERIMENT RESULTS

4.1 Experimental spray image

Figure 12 illustrates the macroscopic development process of methanol spray in different environments. Due to the nozzle comprising an injection surface with 180 tiny orifices, the spray exhibits a large cone angle. When interacting with air, its boundary undergoes rapid and significant surface disintegration. Affected by aerodynamic forces, the momentum of the disintegrated droplets decreases swiftly, resulting in a velocity lag compared to the penetration speed at the spray's leading edge. In the later stages of the spray (after 5 milliseconds), the fragmentation at the spray head becomes highly pronounced. As air entrainment is more significant at the head, the small droplets resulting from the fragmentation of the spray head are widely distributed. It is evident that as the ambient temperature increases (from 298K to 310K), the penetration distance of the methanol spray increases significantly. However, from 310K to 323K, the increase in spray penetration distance is less pronounced.

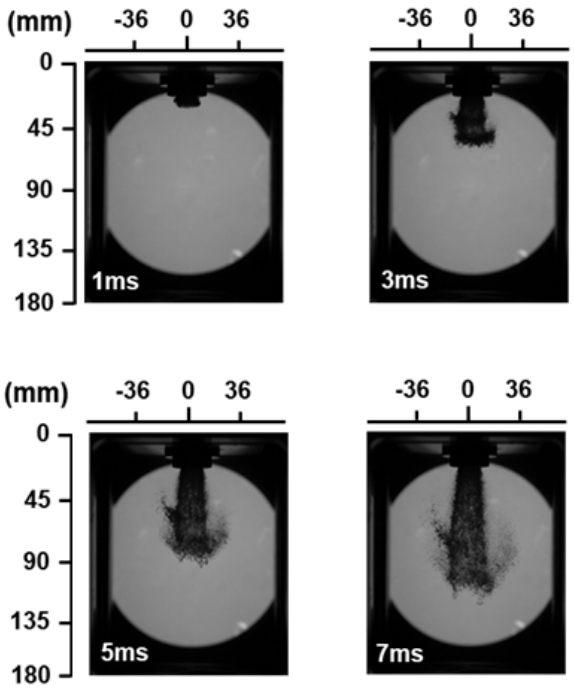

(a) P_{inj}=9 barG, P_{aim}=9 barG, T_{aim}=298 K

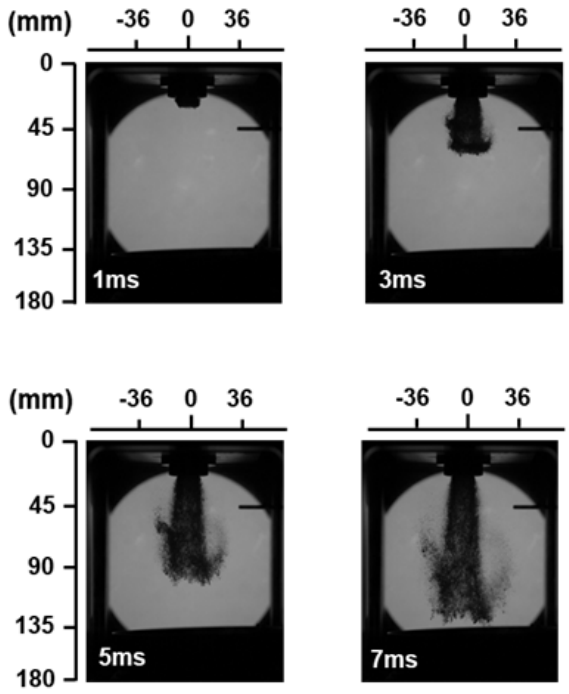

(b) Pinj=9 barG, Paim=3 barG, Taim=310 K

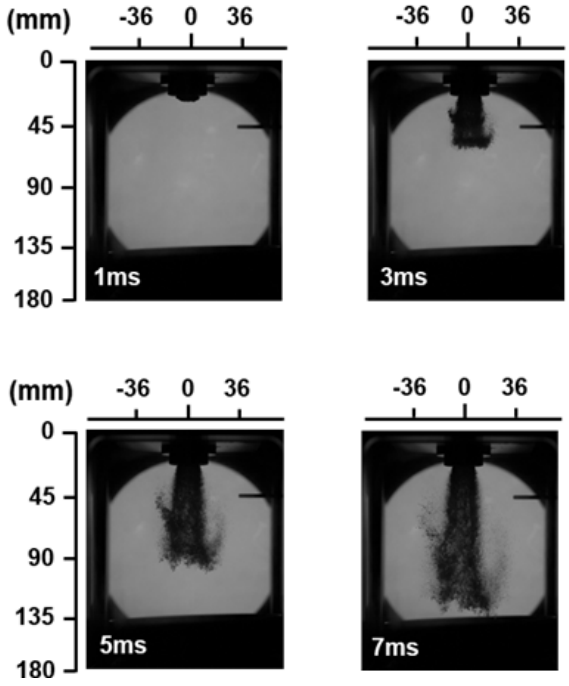

(c) Pinj=9 barG, Paim=3 barG, Taim=323 K

Figure 12. Macroscopic development process of methanol spray at different ambient temperatures

4.2 Characteristics of Spray Penetration Distance and Spray Cone Angle

Figure 13 presents the changes in penetration distance and spray cone angle of methanol spray under different temperature conditions. When the ambient temperature increases from 298K to 323K, the spray penetration distance does not change significantly within the first 3ms after spray initiation. However, beyond 3ms, the methanol spray penetration distance in higher temperature environments increases markedly. The difference in penetration distance between 310K and 323K is minimal, but compared to 298K, the penetration distance increases by nearly 30%. This is primarily due to the decrease in spatial gas density as the ambient temperature increases (from 298K to 323K), which reduces the interaction between the methanol spray and the air, resulting in lower momentum loss for the spray. Consequently, the spray penetration distance at 323K is greater than that at room temperature. It should be noted that as the ambient temperature continues to rise, it significantly promotes endothermic evaporation of methanol and enhances atomization and breakup. At this point, atomization and breakup play a decisive role, and the methanol droplets will interact more strongly with the air, facilitating the formation of the mixture. Meanwhile, it can be observed that as the ambient temperature increases from 298K to 323K, there is no significant difference in spray cone angle among the three operating conditions.

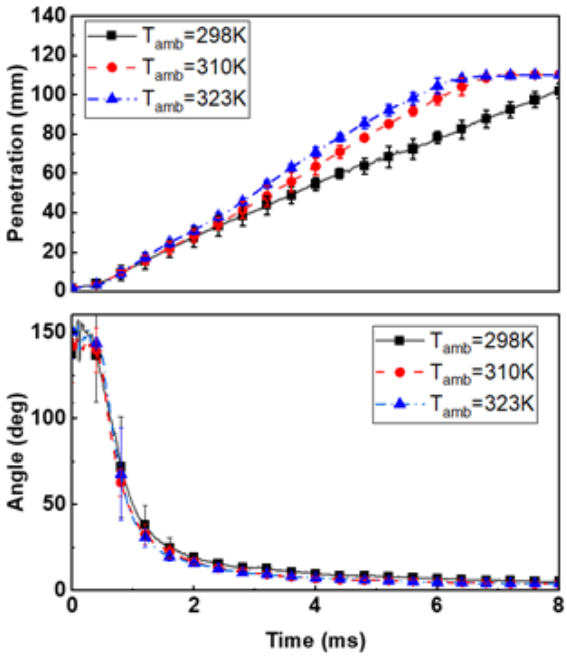

Figure 13. Characteristics of methanol spray penetration distance and spray cone angle at different ambient temperatures

Figure 14 demonstrates the variations in methanol spray penetration distance and spray cone angle under different injection pressures with a fixed pressure difference. It can be observed that, despite the same pressure difference, the lower injection pressure results in a lower backpressure,

leading to a reduced spatial density and decreased interaction between methanol and the ambient gas. Under these conditions, the penetration distance increases significantly. Conversely, at high injection pressures, despite the same pressure difference, the higher ambient backpressure effectively shortens the spray penetration distance by more than 30%. This indicates that maintaining a consistent pressure difference does not guarantee the same penetration distance during methanol port injection, especially at low loads. Due to the higher penetration distance, severe interference between liquid methanol and the intake manifold wall may occur, leading to wet-wall phenomena, uneven mixture formation, increased cyclic variations, and adverse effects on further increasing the substitution rate under low-load conditions. Additionally, the high injection pressure corresponding to high backpressure causes the methanol spray to be significantly compressed, resulting in a wider radial distribution range during the initial spray development stage and a larger initial spray cone angle at an injection pressure of 9barG.

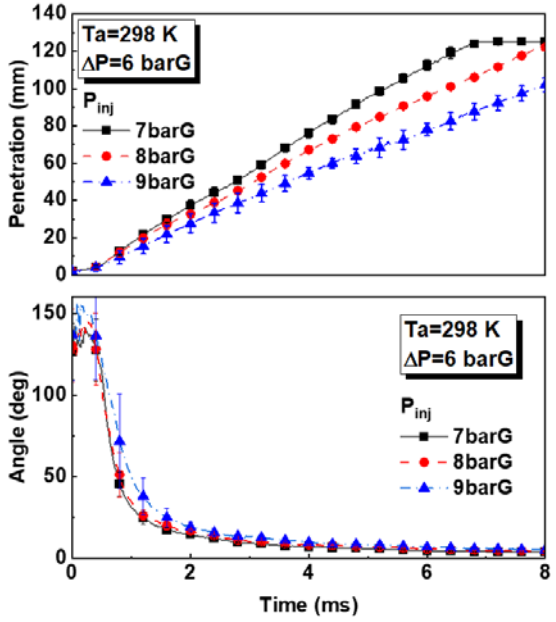

Figure 14. Characteristics of methanol spray penetration distance and spray cone angle under different injection pressures at a fixed pressure difference

4.3 Spray Particle Size Distribution

Figure 15 shows the droplet size distribution characteristics of methanol spray at axial positions of 60mm and 80mm under different ambient temperatures. It can be observed that as the temperature increases from 298K to 323K, the probability of droplet size distribution at 20μm increases from 56.2% to 59.5% at the downstream axial position of 80mm, with an increase of 3.3% points (Pt). However, at the midstream position of 60mm, the probability of droplet size distribution at 20μm decreases from 57.3% to 56.6%, with a decrease of 0.7% points (Pt). This indicates that, due to the temperature increase, atomization improvement first occurs at the head of the methanol spray. It is mainly because air entrainment is most intense at the spray head, and combined with the higher surrounding temperature, the atomization of methanol droplets in this area is affected by temperature earlier. However, in the midstream section, where the entrainment effect is not as intense as at the spray front, the decrease in air density due to the surrounding temperature rise becomes the dominant factor. Consequently, there is less interaction between droplets and air, leading to reduced droplet breakup. As a result, the probability of small droplets at the 60mm position at 323K is lower than that at 298K.

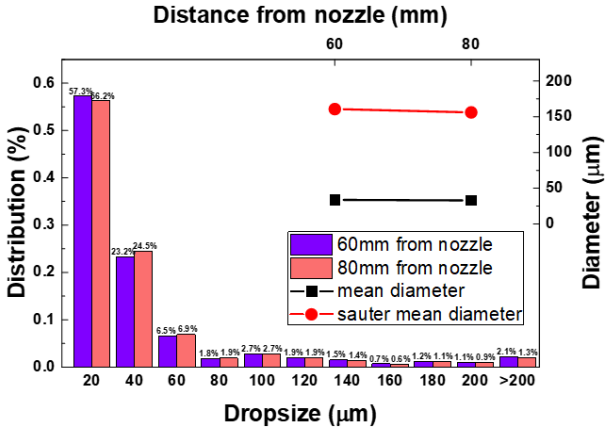

(a) Pinj=9 barG, Paim=3 barG, Taim=298 K

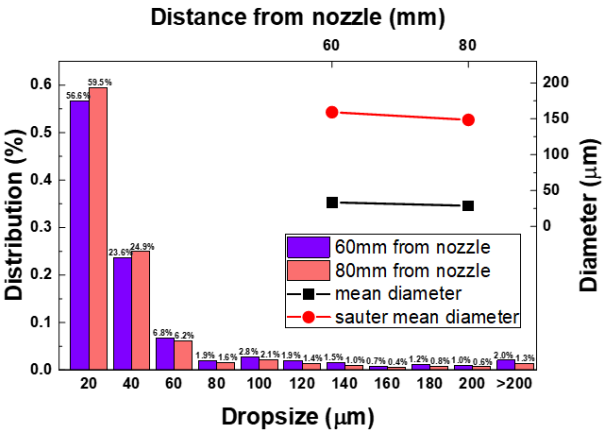

(b) Pinj=9 barG, Paim=3 barG, Taim=323 K

Figure 15. Particle size distribution characteristics of methanol spray at different ambient temperatures

5 CONCLUSIONS

Using optical methods such as high-speed backlight scattering and photomicrography, a series of studies were conducted on the macroscopic morphology and atomized droplet size distribution of liquid methanol spray in a simulated low-pressure methanol injection environment for marine medium-speed engines. The main conclusions obtained are as follows:

(1) Photomicrography can effectively capture the droplet size distribution.

(2) Within the temperature range from 298K to 323K, an increase in temperature lead to a decrease in the density of the ambient gas. At this time, the spray penetration of methanol at 323K was significantly greater than that under normal temperature conditions. This indicated that within a relatively low temperature range, the influence of density changes caused by variations in the ambient gas temperature was more significant than the effect of temperature in promoting methanol atomization.

(3) The front end of the methanol spray was more significantly affected by ambient temperature than the midstream section, and the distribution of small droplet sizes was mainly concentrated in the mid-to-downstream sections. Within an initial temperature increase range of 50K, the front end of the methanol spray was notably affected by ambient temperature, resulting in a denser distribution of small droplet sizes. However, in the midstream section, the main influence was from the decreased density of the surrounding gas, which leads to limited interaction between methanol droplets and the ambient air, restricting atomization and resulting in a lower distribution of small droplet sizes.

(4) Even with the same pressure difference, low backpressure and low injection pressure conditions lead to a significantly higher spray penetration distance compared to high backpressure and high injection pressure conditions. It suggests that low-load conditions are more prone to causing wet-wall phenomena in methanol port injection sprays.

6 DEFINITIONS, ACRONYMS, ABBREVIATIONS

IMO: International Maritime Organization

DBI: Diffused Background Illumination

SA: spray angle

fps: frames per second

7 ACKNOWLEDGMENTS

This study is part of the “Research on Key Technologies of High-Power Methanol-Fueled Low-Speed Engines for Ocean-Going Ships” project which has received funding from the Action Plan for Scientific and Technological Innovation (project number: 23XD1434900).

8 REFERENCES AND BIBLIOGRAPHY

[1] Li, Y.Q. 2023. The Impact of Green and Low-Carbon Practices on the Development of the Maritime Industry, Shipbuilding, 34(04): 1-18.

[2] Wang, M.C., Hong, Z.X., Li, F., et al. 2024. Analysis of the Current Status and Prospects for the Development of the Green Methanol Industry, International Petroleum Economics, 32(05): 78-84.

[3] Zhang, D.M, Shen, X, Wang, L.J, et al. 2023. Current Status and Trends in the Development of Marine Methanol Engine Technology, Diesel Engine, 45(05): 1-4.

[4] Wang, L.J, Zeng, X.G, Qin, Y. Overview of the Development of the Methanol-Fueled Marine Power Vessel Industry Chain [J]. China Ship Survey, 2024, (04): 38-42.

[5] Wu, X.F. 2023. The Status Quo and Supply Chain Analysis of Green Methanol as a Decarbonization Fuel for Shipping, Tianjin Navigation, (03): 74-78.

[6] Heaney, D.F. 2012. Designing for metal injection molding (MIM). Oxford: Woodhead

[7] Heaney, D.F. 2012. Handbook of metal injection molding. Oxford: Woodhead

[8]Migneault, S., Koubaa, A., Erchiqui, F., et al. 2011. Application of micromechanical models to tensile properties of wood-plastic composites, Wood Science and Technology, 45(3): 521-532.

[9] Pickett, L.M., Siebers, D. L. and Idicheria, C. A. 2005. Relationship between ignition processes and the lift-off length of diesel fuel jets, IEEE Transactions on Instrumentation and Measurement, 24(14): 1714-1731.

[10] Edwards, C. F., Siebers, D. L., Hoskin, D. H. 1992. A Study of the Autoignition Process of a Diesel Spray via High Speed Visualization, IEEE Transactions on Instrumentation and Measurement, 31(26): 187-204.

[11] Siebers, D, Higgins, B., Pickett, L. 2002. Flame Lift-Off on Direct-Injection Diesel Fuel Jets: Oxygen Concentration Effects, IEEE Transactions on Instrumentation and Measurement, 11(38): 1490-1509.

[12] Higgins, B. and Siebers, D. 2001. Measurement of the Flame Lift-Off Location on DI Diesel Sprays Using OH Chemiluminescence, Proceedings of the Combustion Institute, 23(46): 739-753.

[13] Siebers, D. and Higgins, B. 2001. Flame Lift-Off on Direct-Injection Diesel Sprays Under Quiescent Conditions, Proceedings of the Combustion Institute, 30(36): 400-421.

[14] Jia, T., Xie, J.T., Cao, Z.J., et al. 2021. Study on In-Cylinder Combustion Characteristics of a Heavy-Duty M100 Methanol Engine, Small Internal Combustion Engine and Vehicle Technique, 50(06): 1-9.

[15] Xu, M. 2015. Research on a Quasi-Dimensional Combustion Model for High-Power Density Diesel Engines, Shanghai: Shanghai Jiao Tong University.

9 CONTACT

Wang Xinran, Master's Degree

Engineering, China Shipbuilding Power Engineering Institute Co., Ltd,

6000119@cspi.net.cn